Inorg. Chem. **2005**, *44*, 6545–6549

Novel Corrugated In_9 Anionic Layer in $Li_2Y_5In_9$: Square Pyramidal In_5 Clusters Interconnected by Unusual Butterfly In_4 Clusters

Zhong-Ming Sun, Jiang-Gao Mao,* and Da-Chun Pan

State Key Laboratory of Structural Chemistry, Fujian Institute of Research on the Structure of Matter, Chinese Academy of Sciences and the Graduate School of Chinese Academy of Sciences, Fuzhou 350002, P. R. China

Received March 28, 2005

The new ternary polar intermetallic phase, $Li_2Y_5In_9$, was obtained by high-temperature solid-state reactions of the corresponding elements inwelded Ta tubes. Its crystal structure was established by a single-crystal X-ray diffraction study. $Li_2Y_5In_9$ crystallizes in the tetragonal space group *P*4/*nmm* (No. 129) with cell parameters of $a = b = 10.1242(4)$, $c = 15.1091(10)$ Å and $Z = 4$. The structure of $Li_2Y_5In_9$ features a two-dimensional corrugated anionic In_9 layer composed of two types of square pyramidal In_5 units and butterfly In_4 units. There are two types of square pyramidal In_5 units: one with normal In–In bonds and another one with greatly elongated In–In separations within its In_4 square. Packing of these 2D In_9 layers resulted in cavities and tunnels that are occupied by Y and Li atoms. Extended-Hückel tight-binding calculations indicate that $Li_2Y_5In_9$ is metallic.

Introduction

Group 13 elements (triels) form a large number of polar intermetallics when alloyed with alkali, alkali earth, or rare earth elements. Among them, gallium and indium generally form extended anionic cluster frameworks, as well as a few examples of discrete clusters, whereas thallium phases are rich in isolated cluster moieties.[1−3] The chemical bonding and electron count for most of above polar intermetallic compounds can be explained by the Zintl−Klemm concept, as well as Wade's rules.[4−6] In the case of indium phases, a number of binary phases with three-dimensional indium networks have been reported, such as $CaIn_2$ and $SrIn_2$,[7,8] Sr_3In_5,[9] $EuIn_4$,[10] $SrIn_4$,[11] and Sr_3In_{11}.[12,13] In addition, binary phases containing isolated or hypoelectronic clusters have also been prepared.[14−17] In some phases, the cluster units are interconnected via exo bonds into a complex network structure. Different from those in La_3In_5, the In_5^{9-} clusters in α-Y_3In_5 are twisted and interconnected by short In−In bonds at trans-basal positions into 1D chains.[15] Other examples include $Na_{15}In_{27.4}$ featuring a 3D network of Na-centered *closo*-In_{16} clusters and *nido*-In_{11} units,[14] $K_{17}In_{41}$ with a 3D network structure based on *closo*-In_{12} and In-centered *closo*-In_{17}.[18] It is worth noting that the 3D indium network in $K_{39}In_{80}$ is composed of three types of empty In_{12} icosahedra with different exo bonding and symmetry, In_{16} icosaoctahedra centered each by a tetrahedral indium, and open In_{15} spacers.[19]

* To whom correspondence should be addressed. E-mail: mjg@ms.fjirsm.ac.cn.

(1) (a) Corbett, J. D. In *Chemistry, Structure and Bonding of Zintl Phases and Ions*; Kauzlarich, S., Ed.; VCH Publishers: New York, 1996; p 139. (b) Corbett, J. D. *Angew. Chem., Int. Ed.* **2000**, *39*, 670. (c) Corbett, J. D. *Chem. Rev.* **1985**, *85*, 383. (d) Corbett, J. D. *Inorg. Chem.* **2000**, *39*, 5178 and references therein.
(2) (a) Belin, C.; Tillard-Charbonnel, M. *Prog. Solid State Chem.* **1993**, *22*, 59. (b) Belin, C.; Tillard-Charbonnel, M. *Coord. Chem. Rev.* **1998**, *178−180*, 529. (c) Tillard-Charbonnel, M.; Manteghetti, A.; Belin, C. *Inorg. Chem.* **2000**, *39*, 1684. (d) Miller, G. J. In *Chemistry, Structure and Bonding in Zintl Phases and Ions*; Kauzlarich, S., Ed.; VCH Publishers: New York, 1996; p 1. (e) Eisenmann, B.; Cordier, G. In *Chemistry, Structure and Bonding in Zintl Phases and Ions*; Kauzlarich, S., Ed.; VCH Publishers: New York, 1996; p 61 and references therein.
(3) (a) Dong, Z.-C.; Corbett, J. D. *J. Cluster Sci.* **1995**, *6*, 187. (b) Dong, Z.-C.; Corbett, J. D. *J. Am. Chem.* Soc. **1993**, *115*, 11299. (c) Dong, Z.-C.; Corbett, J. D. *J. Am. Chem. Soc.* **1994**, *116*, 3429.
(4) (a) Nesper, R. *Angew. Chem., Int. Ed. Engl.* **1991**, *30*, 789. (b) Nesper, R. *Prog. Solid State Chem.* **1990**, *20*, 1.
(5) (a) Zintl, E. *Angew Chem.* **1939**, *52*, 1. (b) Klemm, W.; Busmann, E. *Z. Anorg. Allg. Chem.* **1963**, *319*, 297.
(6) Wade, K. *Adv. Inorg. Chem. Radiochem.* **1976**, *18*, 1.
(7) Nuspl, G.; Polborn, K.; Evers, J.; Landrum, G. A.; Hoffmann, R. *Inorg. Chem.* **1996**, *35*, 6922.
(8) Wendorff, M.; Röhr, C. *Z. Anorg. Allg. Chem.* **2005**, *631*, 338.
(9) Seo, D. K.; Corbett, J. D. *J. Am. Chem. Soc.* **2001**, *123*, 4512.
(10) Fornasini, M. L.; Ciafici, S. *Z. Kristallogr.* **1990**, *190*, 295.
(11) Seo, D. K.; Corbett, J. D. *J. Am. Chem. Soc.* **2000**, *122*, 9621.
(12) Amerioun, S.; Häussermann, U. *Inorg. Chem.* **2003**, *42*, 7782.
(13) Mao, J.-G.; Guloy, A. M. *J. Alloys Compds.* **2004**, *363*, 143.
(14) Sevov, S. C.; Corbett, J. D. *J. Solid State Chem.* **1993**, *103*, 114.
(15) Zhao, J.-T.; Corbett J. D. *Inorg. Chem.* **1995**, *34*, 378.
(16) Sevov, S. C.; Corbett, J. D. *Inorg. Chem.* **1991**, *30*, 4875.
(17) Blase, W.; Cordier, G.; Somer, M. *Z. Kristallogr.* **1991**, *194*, 150.
(18) Cordier, G.; Müller, V. *Z. Kristallogr.* 1993, *205*, 353.

10.1021/ic050462j CCC: $30.25
Published on Web 08/23/2005

The use of mixed cations with different sizes or/and different charges has led to the discovery of many novel phases which cannot be prepared by using either type of cations. The success of this synthetic route can be attributed to the lessening of the cation-packing limitations and the electronic requirements. Some examples of mixed-cation indium phases are $K_{14}Na_{20}In_{96.30}$ in which two In_{28} clusters are linked by two In atoms into a $(In_{28})In_2(In_{28})$ sandwich unit,[20] $A_3Na_{26}In_{48}$ (A = K, Rb, Cs) with a novel cubic network of *arachno*- and *closo*-In_{12},[21,22] $K_{18.2}Na_{4.8}In_{39}$ containing *closo*-In_{12} plus an In_{15} spacer in $K_{18.2}Na_{4.8}In_{39}$,[23] and KNa_3In_9 composed of *closo*-In_{12} clusters plus four-bonded In atoms.[24] Two examples in which the two types of cations have different charges are $Ca_{18}Li_5In_{25.07}$, featuring the intergrowth of defect cluster layers of Li-centered In_{12} icosahedra (8-exo-bonds) with electron-precising In_3^{5-} Zintl layers,[25] and K_2SrIn_7 with a remarkable electron-deficient indium network.[26]

It is hoped that the combination of the alkali metal (A), such as lithium, and the rare earth (RE) metal, such as yttrium, which are different in both size and charge, can lead to novel ternary indium phases with unusual indium anionic clusters or networks. So far, none of such compounds has been reported. Herein, we report the synthesis, crystal structure, and chemical bonding of a new ternary polar intermetallic phase, $Li_2Y_5In_9$, whose structure features a two-dimensional In_9 anionic layer composed of two types of square pyramidal In_5 units that are bridged by the unusual butterfly In_4 units.

Experimental section

Synthesis. All manipulations were performed inside an argon-filled glovebox with moisture level below 1 ppm. The starting materials were lithium ingot (99.9%, Aldrich), yttrium pieces (99.9%, Alfa), and indium powder (99.99%, Aldrich). Single crystals of $Li_2Y_5In_9$ were initially obtained by solid-state reaction of lithium (0.014 g, 2.0 mmol), yttrium (0.133 g, 1.5 mmol), and indium (0.344 g, 3.0 mmol). The mixture was loaded into a tantalum tube, which was then sealed in a quartz tube under vacuum ($\sim 10^{-4}$ Torr). It was put into an oven and heated at 960 °C for 48 h and annealed at 700 °C for 15 days. Afterward, it was allowed to cool at a rate of 0.1 °C/min to room temperature. Silver-gray crystals of $Li_2Y_5In_9$ were obtained. Several single crystals were analyzed by the energy-dispersive X-ray spectroscopy (EDAX 9100), and results confirmed the presence of Y and In elements in a ratio of 0.53:1.0, which is in good agreement with the results from single-crystal structure refinements. After the structural analysis, a lot of efforts were subsequently made to prepare a single phase of $Li_2Y_5In_9$. The reactions were carried out with a stoichiometric mixture of the elements, as well as using of an excess of 10∼20% lithium to compensate its possible loss during arc-welding. The samples were heated at 980 °C for 48 h, quenched in water, and annealing at different temperatures (600, 650, 700, 750, and 800 °C, respectively, for each individual reaction) for as long as one month; however, XRD powder patterns of the resultant products revealed the presence of indium elements (tetragonal phase), as well as other unidentified impurities, in addition to the major phase of $Li_2Y_5In_9$ (∼80%). The highest yield (∼80%) was obtained by annealing at 700 °C; annealing at temperatures lower or higher than 700 °C will significantly decrease the yield. Attempts were also made to prepare the analogues of other lanthanide elements, such as La and Sm, by using similar conditions to that for $Li_2Y_5In_9$. XRD powder studies for the products revealed the presence of Li_3In_2 (*R-3m*) and La_3In_5 (or Sm_3In_5 in *Cmcm*) as major phases but showed no evidences for the formation of $Li_2Ln_5In_9$ (Ln = La, Sm) phases, which is probably due to the too-large ionic sizes of these two lanthanide elements.

Table 1. Summary of Cell Parameters, Data Collection, and Structure Refinements for $Li_2Y_5In_9$

empirical formula	$Li_2Y_5In_9$
fw	1491.81
space group	*P*4/*nmm* (No. 129)
a, Å	10.1242(4)
c, Å	15.109(1)
V, Å^3	1548.7(1)
Z	4
D_{calcd}, g cm^{-3}	6.398
temp, K	293(2)
μ, mm^{-1}	31.556
GOF on F^2	1.168
R1, wR2 ($I > 2\sigma(I)$)[a]	0.0320/0.0528
R1, wR2 (all data)	0.0384/0.0546

[a] $R1 = \sum||F_o| - |F_c||/\sum|F_o|$, $wR2 = \{\sum w[(F_o)^2 - (F_c)^2]^2/\sum w[(F_o)^2]^2\}^{1/2}$.

Crystal Structure Determination. A silver-gray single crystal of $Li_2Y_5In_9$ with a dimension of 0.12 × 0.12 × 0.06 mm^3 was selected from the reaction product and sealed into a thin-walled glass capillary under an argon atmosphere. Data collection was performed on a Rigaku Mercury CCD (MoKα radiation, graphite monochromator) at 293(2) K. The data set was corrected for the Lorentz factor, polarization, air absorption, and absorption due to variations in the path length through the detector faceplate. Absorption correction based on the multiscan method was also applied.[27]

The space group for $Li_2Y_5In_9$ was uniquely determined to be *P*4/*nmm* (No. 129) on the basis of systematic absences, *E*-value statistics, and the satisfactory refinements for the structure. The structure was solved by using direct methods (SHELXTL) and refined by least-squares methods with atomic coordinates and anisotropic thermal parameters.[28] The thermal parameters for Y(1) and Y(4) are larger than those of Y(2) and Y(3); however, results of occupancy factor refinements gave no indication of mixing of these two Y atoms with Li atom. Y(1) and Y(4) atoms show elongated thermal ellipsoids for U_{33}, which is probably due to several longer Y−In bonds (Y(1)−In(1) = 3.326(2) Å and Y(4)−In(4) = 3.417(2) Å). All Y and In sites are fully occupied according to the site occupancy refinements. Final difference Fourier maps showed featureless residual peaks of 2.230 and −1.926 eÅ^{-3} (both within 1.0 Å of In(5) atom). Some of the data collection and refinement parameters are summarized in Table 1; the atomic coordinates, and important bond lengths are listed in Tables 2 and 3, respectively. More details of the crystallographic studies, selected

(19) Li, B.; Corbett, J. D. *Inorg. Chem.* **2003**, *42*, 8768.
(20) Li, B.; Corbett, J. D. *J. Am. Chem. Soc.* **2005**, *127*, 926.
(21) Sevov, S. C.; Corbett, J. D. *Inorg. Chem.* **1993**, *32*, 1612.
(22) Carrillo-Cabrera, W.; Caroca-Canales, N.; Peters, K.; von Schnering, H.-G. *Z. Anorg. Allg. Chem.* **1993**, *619*, 1556.
(23) Carrillo-Cabrera, W.; Caroca-Canales, N.; von Schnering, H.-G. *Z. Anorg. Allg. Chem.* **1994**, *620*, 247.
(24) Li, B.; Corbett, J. D. *Inorg. Chem.* **2002**, *41*, 3944.
(25) Mao, J.-G.; Goodey, J.; Guloy, A. M. *Inorg. Chem.* **2004**, *43*, 282.
(26) Chi, L.-S.; Corbett, J. D. *Inorg. Chem.* **2001**, *40*, 3596.
(27) *CrystalClear*, version 1.3.5; Rigaku Corp.: Woodlands, TX, 1999.
(28) Sheldrick, G. M. *SHELXTL*, version 5.03; Siemens Analytical X-ray Instructuments, Madison, WI, 1995; Sheldrick, G. M. *SHELX-96 Program for Crystal Structure Determination*, 1996.

Table 2. Atomic Coordinates and U_{eq} ($\times 10^3$ Å^2) for $Li_2Y_5In_9$

atom	site symm.	*x*	*y*	*z*	U_{eq}[a]
Y(1)	2c	1/4	1/4	0.1684(2)	22(1)
Y(2)	8j	0.4690(1)	0.0310(1)	0.3734(1)	8(1)
Y(3)	8j	0.5332(1)	0.9669(1)	0.1275(1)	8(1)
Y(4)	2c	3/4	3/4	0.3055(2)	16(1)
Li(1)	4f	3/4	1/4	0.101(2)	28(6)
Li(2)	4f	3/4	1/4	0.409(2)	28(6)
In(1)	8i	0.4992(1)	1/4	0.0249(1)	14(1)
In(2)	2c	1/4	1/4	0.3806(1)	17(1)
In(3)	8i	0.5419(1)	1/4	0.2312(1)	10(1)
In(4)	8i	0.4779(1)	1/4	0.5277(1)	11(1)
In(5)	2c	3/4	3/4	0.0946(1)	17(1)
In(6)	8i	3/4	0.4501(1)	0.2687(1)	10(1)

[a] U_{eq} is defined as one-third of the trace of the orthogonalized U_{ij} tensor.

Table 3. Selected Bond Lengths (Å) for $Li_2Y_5In_9$

Y(1)−In(3)	3.103(1) × 4	Y(1)−In(2)	3.206(3)
Y(1)−In(1)	3.326(2) × 4	Y(2)−In(2)	3.1378(9)
Y(2)−In(3)	3.1746(8) × 2	Y(2)−In(4)	3.2191(9) × 2
Y(2)−In(4)	3.2581(8) × 2	Y(2)−In(6)	3.2605(7) × 2
Y(2)−Li(2)	3.647(4) × 2	Y(2)−Y(3)	3.827(1)
Y(3)−In(5)	3.144(1)	Y(3)−In(6)	3.1747(8) × 2
Y(3)−In(1)	3.1977(9) × 2	Y(3)−In(3)	3.2680(8) × 2
Y(3)−In(1)	3.2770(8) × 2	Y(3)−Li(1)	3.633(4) × 2
Y(3)−Y(2)	3.827(1)	Y(4)−In(6)	3.0870(8) × 4
Y(4)−In(5)	3.186(3)	Y(4)−In(4)	3.417(2) × 4
Li(1)−In(1)	2.79(1) × 2	Li(1)−In(3)	2.88(2) × 2
Li(1)−Li(1)	3.05(6)	Li(2)−Li(2)	2.75(5)
Li(2)−In(4)	2.917(9) × 2	Li(2)−In(6)	2.93(2) × 2
In(1)−In(5)	3.102(1)	In(1)−In(3)	3.146(1)
In(2)−In(4)	3.203(1) × 4	In(3)−In(6)	2.9774(7) × 2
In(4)−In(6)	3.1619(9)	In(4)−In(4)	3.263(1) × 2
In(5)−In(1)	3.102(1) × 4	In(6)−In(3)	2.9774(7)
In(6)−In(4)	3.1619(9)	In(1)...In(1)	3.567(1) × 4
In(6)...In(6)	4.051(1)	In(3)...In(3)	4.214(1)
In(1)...In(1)	3.670(1)		

bond angles, and atomic displacement parameters are given in the Supporting Information.

Band Structure. Three-dimensional band structure calculations for $Li_2Y_5In_9$, along with the density of states (DOS) and crystal orbital overlap population (COOP) curves, were performed using the Crystal and Electronic Structure Analyzer (CAESAR) software package.[29] The following atomic orbital energies were employed for the calculations: Y 5s, −6.61; 5p, −4.18; 4d, −6.27; Li 2s, −5.4; 2p, −3.5; In 5s, −12.6; 5p, −6.19 eV.[29, 30]

Results and discussion

The ternary phase, $Li_2Y_5In_9$, belongs to a new structure type. Its structure features a corrugated two-dimensional In_9 anionic layer composed of two types of square pyramidal In_5 units bridged by the butterfly In_4 units via In−In exo bonds.

There are six indium atoms in an asymmetric unit of $Li_2Y_5In_9$. They form three types of cluster units (Figure 1a): two types of well-defined square pyramidal In_5 units and the butterfly In_4 unit. In(2) and 4 In(4) atoms form a square pyramidal In_5 unit (C_{4v}). The four In(4) atoms form the planar In_4 square with In−In distance of 3.263(1) Å, whereas the In(2) atom occupies the pyramidal site. The In(2)−In(4) distance of 3.203(1) Å is slightly shorter than the In(4)−In(4) bonds. These In−In bonds are significantly longer than that of the Pauling single bond (~2.96 Å)[31] but are comparable to those reported in other indium phases.[8−26] The nearest In−In distance between neighboring In_5 cluster units is 3.985 (1) Å, which is much longer than those in La_3In_5 and Y_3In_5.[15] It should be mentioned that the square pyramidal In_5 units in La_3In_5 (C_{2v}), α-Y_3In_5 (C_s), and β-Y_3In_5 (C_{2v}) are distorted and have a lower symmetry.[15] It is also interesting to note that the In_5 cluster unit in $Ba_{19}In_9N_9$ adopts the trigonal bipyramidal geometry.[32] One In(5) and four In(1)

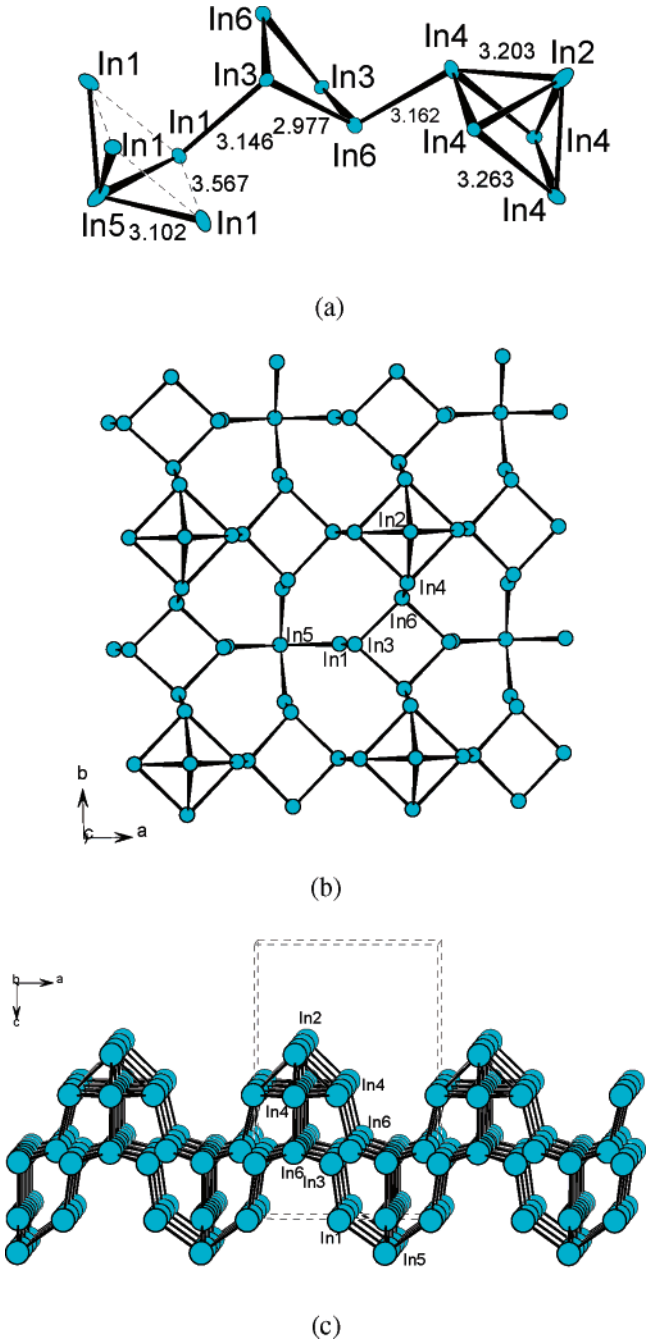

Figure 1. The square pyramidal In_5 and unusual butterfly In_4 units (a) and view of the In_9 anionic layer in $Li_2Y_5In_9$ along *c* (b) and *b* axes (c). The thermal ellipsoids are drawn at 75% probability.

(29) Ren, J.; Liang, W.; Whangbo, M.-H. *CAESAR for windows*; Prime-Color Software, Inc., North Carolina State University: Raleigh, NC, 1998.
(30) Maggard, P. A.; Corbett, J. D. *Inorg. Chem.* **2004**, *43*, 2556.
(31) Pauling, L. *The Nature of the Chemical Bond*; Cornell University Press: Ithaca, NY, 1960; p 400.

atoms form the second type of square pyramidal In_5 unit, also with C_{4v} symmetry. The In(5)−In(1) distance of 3.102 Å is slightly shorter than that of In(2)−In(4). In−In distances within the square plane are 3.567(1) Å, which are very weak bonds according to band structure calculations (with an average overlap population (OP) value of ∼0.06); however, we can still consider this In_5 unit to be a square pyramid for the topological reason. The In(1)−In(5)−In(1) bond angles (70.20(3)° and 108.82(6)°) are also significantly larger than those of the corresponding In(4)−In(2)−In(4) ones (61.23(3) and 92.15(5)°). Two In(3) and two In(6) atoms form a butterfly In_4 unit (C_{2v}). The In(6) atoms lie along the fold of the wings (In(6)···In(6) = 4.051(1) Å) and the In(3) atoms act as the wings (In(3)···In(3) = 4.214(1) Å). The In(3)−In(6) distance of 2.9775(7) Å is significantly shorter than those for the above In_5 units. The folding angle defined as the dihedral angle between the two wing planes is 30.1°. The In(6)−In(3)−In(6) angle of 85.74(3)° is significantly deviated from 90° for a square planar In_4 unit. Such geometry lies between tetrahedron and square planar, and similar butterfly units were reported in $In_2Se_2^{2-}$ and $In_2Te_2^{2-}$.[33]

The above In_5 units are bridged by butterfly In_4 units into a 2D In_9 corrugated layer that is normal to the *c* axis via intercluster bonds (Figure 1b and c). Each butterfly In_4 unit bridges with two normal and two elongated square pyramidal In_5 units via four exo bonds. Likewise, each In_5 unit connects with four butterfly In_4 units by using its four square indium atoms. The exo bonds are 3.162(1) and 3.146(1) Å, respectively. The butterfly In_4 units are located at the center of the layer, and they are arranged alternatively up and down along *a* axis. The square pyramidal In_5 units are located at both sides of the layer (Figure 1c). The shortest In···In separation between two In_5 units from two neighboring layers is 3.670(1) Å; results of band structure calculations indicate that it is a very weak bond with an OP value of 0.044. Neighboring In_9 layers are held together by Y and Li atoms through Y−In and Li−In bonds, resulting in a complex 3D network (Figure 2). Viewing down the *c* axis, there are two types of tunnels along *c* axis (Figure 2b). The small ones are composed of In_4 four-member rings and are occupied by the lithium atoms, whereas the large ones are created by butterfly In_4 units and square pyramidal In_5 units, which are occupied by Y(2) and Y(3) atoms. The other yttrium atoms, Y(1) and Y(4), are located at interlayer cavities (Figure 2b).

All four yttrium atoms are 9-coordinated by nine In atoms in a monocapped tetragonal prismatic geometry. Y(1) is surround by one In(2), four In(1), and four In(3) atoms. Y(2) is coordinated by one In(2), two In(3), four In(4), and two In(6) atoms. Y(3) is in contact with four In(1), two In(3), one In(5), and two In(6) atoms. The Y(4)In_9 polyhedron contains four In(4), one In(5), and four In(6) atoms (see Supporting Information, Figure S3). The Y−In distances are in the range of 3.0870(8)−3.417(2) Å (Table 3), which are comparable to those in Y_3In_5.[14] The In−Y−In bond angles

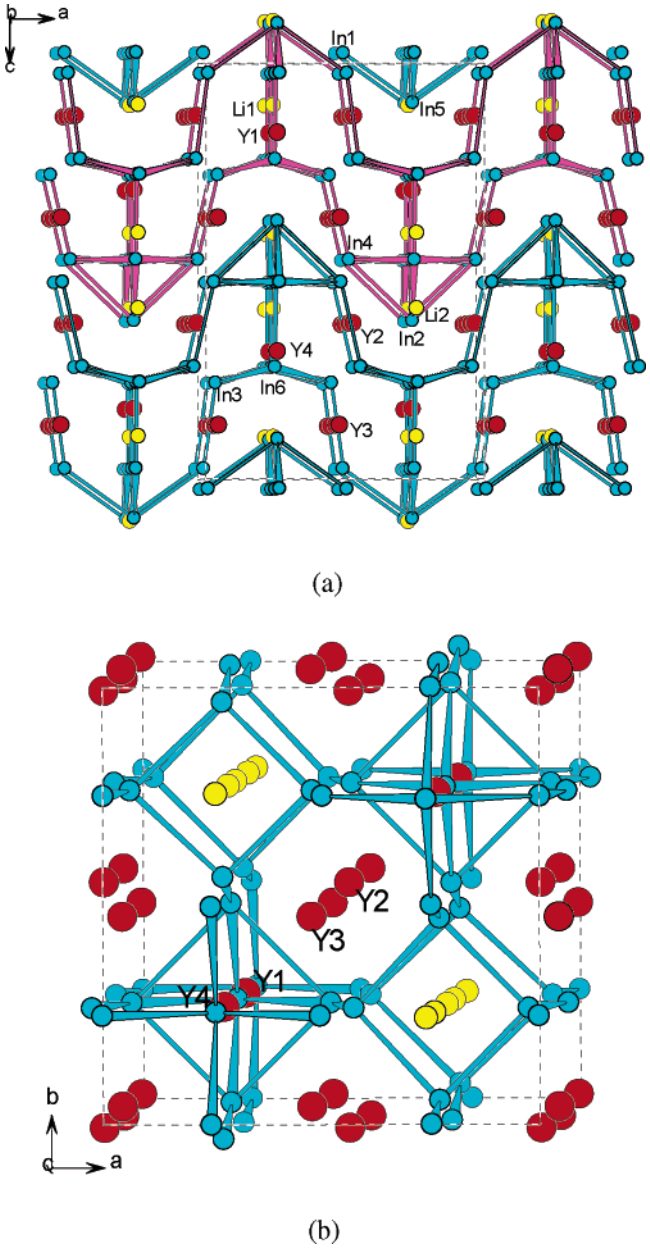

Figure 2. View of the structure of $Li_2Y_5In_9$ along the *b* (a) and *c* (b) axes. Y, Li, and In atoms are represented by red, yellow, and cyan circles, respectively.

vary from 55.03(2) to 162.56(3)°. The shortest Y···Y separation is 3.827(1) Å. Both Li atoms are surrounded by four In atoms in a severely distorted square planar geometry. Li(1) is 4-coordinated by two In(1) and two In(3) atoms with Li−In distances of 2.789(2) and 2.881(2) Å, respectively. The Li(2) atom is surrounded by two In(4) and two In(6) atoms with Li−In distances of 2.916(2)−2.932(2) Å (Table 3). The In−Li−In bond angles are in the range of 65.5(1)−161(1) °, which are significantly deviated from 90° and 180° for an ideal square planar $LiIn_4$ unit. The shortest Y−Li and Li−Li contacts are 3.633(4) and 2.75(5) Å, respectively.

The six crystallographically unique indium atoms have different coordination geometries. In(1) is in contact with two In atoms, one lithium, and five yttrium atoms, and In(4) is bonded to four In neighbors, as well as one lithium and five yttrium atoms. Both In(2) and In(5) atoms have four

(32) Yamane, H.; Sasaki, S.; Kajiwara, T.; Yamada, T.; Shimada, M. *Acta Crystallogr.* **2004**, E60: I120.
(33) Borrmann, H.; Campbell, J.; Dixon, D. A.; Mercier, H. P. A.; Pirani, A. M.; Schrobilgen, G. J. *Inorg.* Chem. **1998**, *37*, 1929.

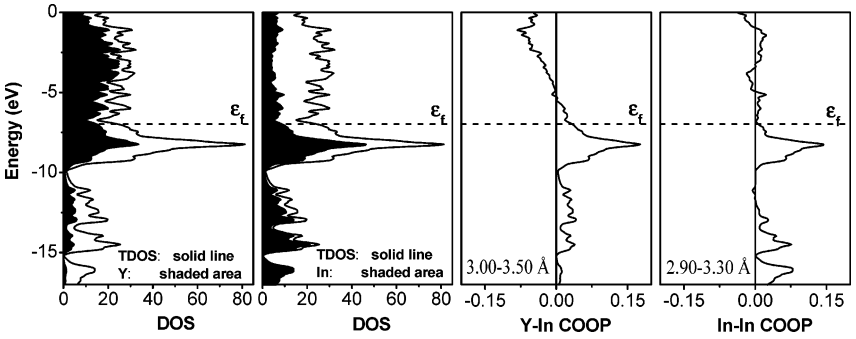

Figure 3. Density of states (DOS) and crystal orbital overlap population (COOP) curves for $Li_2Y_5In_9$. The Fermi level is set at −6.97 eV.

indium and five yttrium atoms as nearest neighbors, whereas In(3) and In(6) atoms are surrounded by three In, one Li, and five Y atoms.

To understand the chemical bonding of $Li_2Y_5In_9$, three-dimensional band structure calculations have been performed by using the CAESAR program.[29] The DOS and COOP curves are presented in Figure 3. There is no observable band gap around the Fermi level, indicating that the compound is metallic. The states just below and above the Fermi level are predominately from 5p states of the indium atoms and 5d states of the yttrium atoms. The contribution from lithium atoms to the DOS states around the Fermi level is very small. The COOP curves are more informative. Both Y−In and In−In interactions are significantly bonding. The average OP values for In−In (2.90−3.5 Å) and Y−Ln (<3.5 Å) are 0.322 and 0.338, respectively. The intracluster In−In contacts for the elongated indium square of the second-type $\{In_5\}$ clusters (3.568 Å) are very weak bonding with an average OP value of 0.06. The interlayer In···In distance of 3.670(1) Å is also a very weak bond with an average OP value of 0.044. The Li−In and Li−Li interactions are essentially nonbonding with small OP values of 0.03 and −0.02, respectively. The calculated Mulliken charges are +0.92 for Li(1), +0.96 for Li(2), and +0.80, +0.39, +0.38, and +0.76 for Y(1), Y(2), Y(3), and Y(4), respectively; hence, the Li atoms almost completely transfer their electrons to the In_9 anionic layer, whereas the yttrium atoms are significantly involved in bonding interactions with the indium layer. For comparison, a Mulliken charge of +0.27 was reported for the Y atoms in $Y_{12}Co_5Bi$ with significant Y−Y, Y−Co, and Y−Bi bonding.[34] Results of our calculations indicate that the strong Y−In, as well as weak interlayer and intracluster In−In bonding interactions, are mainly responsible for the metallic behavior of $Li_2Y_5In_9$.

Conclusion

In summary, a new polar intermetallic phase, $Li_2Y_5In_9$, has been synthesized and structurally characterized. It structure features a corrugated 2D In_9 anion layer, in which two distinct types of square pyramidal In_5 units are bridged by novel butterfly In_4 clusters. The chemical bonding in $Li_2Y_5In_9$ is mainly Y−In and In−In bonding interactions. Our present work further demonstrates that using two types of cations with different charges and atomic sizes is a very effective route to novel polar intermetallic phases.

Acknowledgment. This work is supported by National Natural Science Foundation of China (No. 20371047) and NSF of Fujian Province (No. E0420003).

Supporting Information Available: Figures showing the coordination geometries around Li, Y, and In atoms; lists of selected bond angles; atom displacement parameters; and X-ray crystallographic files for $Li_2Y_5In_9$ in CIF format. This material is available free of charge via the Internet at http://pubs.acs.org.

IC050462J

(34) Tkachuk, A. V.; Mar, A. *Inorg. Chem.* **2005**, *44*, 2272.